

# EFFECTS OF FLOW SCALE ON THE INTERMITTENT PROPERTIES OF A SINGLE STREAM SHEAR LAYER

**Aren M. Hellum**

Department of Mechanical Engineering,  
Michigan State University  
East Lansing, Michigan  
hellumar@egr.msu.edu

**John F. Foss**

Department of Mechanical Engineering,  
Michigan State University  
East Lansing, Michigan  
foss@egr.msu.edu

## ABSTRACT

A four-sensor vorticity ( $\omega_z$ ) probe has been used to characterize the external intermittency in a self-preserving single-stream shear layer at two downstream locations:  $x/\theta_0 = 200, 500$ . The algorithm to define intermittency state as "on" (the mixed, "interior" fluid of the shear layer) or "off" (the exterior fluid of the sheared region's adjacent potential streams) is based on the "activity level" of the  $\omega_z(t)$  time series. This discrimination technique leads to an intermittency time series,  $I(t)$ , with well-defined 1,0 states for the interior and exterior states, respectively. This time series allows conditional statistics for the velocity components to be acquired. Relatively minor differences are observed for the statistical values at the two downstream locations, except for a distinctly lower mean intermittency at  $x/\theta_0 = 500$ . A distinctive result, revealed by the joint histogram of  $u'$ ,  $v'$  for the inactive fluid, is the clear evidence for separate "wedges" of inactive fluid from both the high-speed and low-speed sides of the shear layer. Direct comparisons are made to the 1970 results of Wygnanski and Fiedler.

## INTRODUCTION

External<sup>1</sup> intermittency is present in turbulent flows with one or more "free-stream boundaries". A turbulent boundary layer that is bordered by a shear-free external flow is one example. The single-stream shear layer, studied here, is a second example and it is one with two intermittent regions (high and low-speed sides).

An intermittency function,  $I(t)$ , is assigned to a given location at which the qualitatively different states representing: i) the "interior" (turbulent, vortical, thermally marked, etc.) fluid and ii) the exterior fluid (which lacks those defining qualities), alternatively occupy the given location. Corrsin and Kistler (1955), following the 1943 discovery of this phenomenon by Corrsin, used "vorticity fluctuations" as the defining quantity for the interior fluid. Townsend, as reported in his 1956 monograph, used  $(\partial u/\partial x)^2$  as the conditioning signal to divide time series data into the interior/exterior segments.

---

<sup>1</sup>"External" is in contradistinction with respect to "internal" for the description of "intermittency". The latter represents the high Reynolds number condition in which dissipative regions appear in concentrated "patches" within a fully turbulent flow field.

The associated "viscous superlayer (vsl)" – the propagating membrane-like covering of the interior fluid – can be rationally associated with the vorticity transport equation:

$$\frac{Du}{Dt} = \vec{\omega} \cdot \nabla \vec{V} + \nu \nabla^2 \vec{\omega} \quad (1)$$

Since an irrotational external fluid element can only gain vorticity through the direct action of viscosity and since the "small" value of  $\nu$  for a "large" Reynolds number implies a small length scale for the  $\nabla^2$  operator, it is inferred that the vsl occupies a narrow domain in space. That is, that the width of the vsl scales on the Kolmogorov length of the interior fluid. This observation argues for a designation of  $I(t)$  based upon the presence or absence of vortical fluid at the observation location. Such a designation is rational if the external streams are truly irrotational. The design of the present flow system, as detailed in Morris and Foss (2003), does provide this pristine condition.

Parasitic sensitivity effects, as detailed in Wallace and Foss (1995), showed that the four-sensor  $\omega_x$  probe utilized by Corrsin and Kistler (1955) did not provide an adequate signal for the desired  $I(t)$  discrimination. Subsequent studies by Wygnanski and Fiedler (1969) and (1970), utilized the surrogate signals provided by time derivatives of  $u$  as  $(\partial u/\partial t)^2 + (\partial^2 u/\partial t^2)^2$  with appropriate thresholds to define the  $I=0, 1$  conditions. Hedley and Keffer (1974) expanded upon this approach with the addition of time derivatives of  $v(t)$ . The rationale, in both cases, was to discriminate on the basis of the small scale motions that should represent the vortical fluid state.

The basic probe utilized herein: a four-sensor transverse vorticity probe (Wallace and Foss (1995)), albeit with a less sophisticated computing algorithm, was utilized by Haw, et al. (1989) with the intent to allow the magnitude of  $\omega_z$  to be the defining measure for the  $I=0, 1$  discrimination. Distinct regions of the  $\omega_z(t)$  time series, in which relatively large  $\omega_z(t)$  values were present with quite small fluctuation levels, prompted those authors to adopt an "activity intermittency" designation that is related to the present discrimination technique as discussed in the fourth section.

The present investigation was initiated with the intention to utilize the magnitude of  $\omega_z(t)$  as the conditioning variable for  $I(t)$ . It has subsequently been realized that a substantially more sophisticated understanding of the low-level and low-frequency  $\omega_z(t)$  signals will be required to utilize this in-

principle conditioning scheme. Hence, that utilization will be deferred to a later publication.

An examination of the present  $\omega_z(t)$  data and the consideration of how to best characterize the interior/exterior states within the constraints of available discrimination algorithms has led the present authors to return to the "activity intermittency" designation. Some refinements in the processing algorithm to obtain  $\omega_z(t)$  from the four simultaneously sampled voltages have, however, led to a more refined discrimination process for the intermittency function. The present algorithm for  $I(t)$  is presented in the fourth section.

### THE SUBJECT FLOW FIELD

The large single stream shear layer of Morris and Foss (2003) provided the subject flow field for this investigation; it is represented in plan view in Figure 1. The depth, into the plane of the image, was 2m. The  $R_\theta$  value for the separating boundary layer was  $4.40 \times 10^4$ . The current data were acquired at  $x/\theta_0 = 200$  and 500 for which  $U_0\theta(x)/\nu = 3.36 \times 10^4$  and  $8.40 \times 10^4$ . The flow system's turbulence manipulators delivered irrotational fluid to the high and low speed side entrainment regions. The flows, from the four large fans of the entrainment stream, were adjusted to provide  $dU_0/dx = 0$ . The essential benefit of this flow field is that its large size allows the  $\approx 1mm$  probe domain to appear "small". This can be quantified by the ratio  $\ell^* = \Delta y/\eta_{KOL}$ , where  $\Delta y$  is a characteristic length of the probe (described in the next section) and  $\eta_{KOL}$  is the Kolmogorov length scale near  $\eta = 0$ . For these data,  $\ell^* = 5.32, 3.96$  for  $x/\theta_0 = 200, 500$ , respectively.

### TRANSVERSE VORTICITY MEASUREMENTS

Figure 2 provides a schematic representation of the transverse vorticity probe as previously described in Wallace and Foss (1995). Succinctly stated, the processing algorithm develops a microcirculation domain (length  $\Delta s$  height  $\Delta y$ ) by accumulating convected steps ( $\delta s_k$ ) with incremental time steps ( $\delta t_k$ ). The algorithm determines the circulation

$$\Delta\Gamma = \oint \vec{V} \cdot d\vec{s} \quad (2)$$

for the indicated domain and it then determines the spatially averaged vorticity

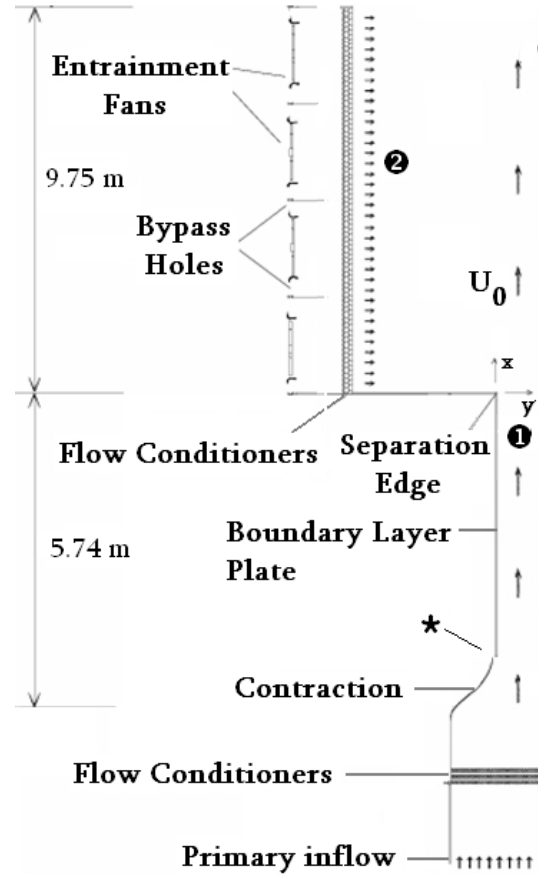
$$\omega_z = \frac{\Delta\Gamma}{(\Delta s)(\Delta y)} \quad (3)$$

for the nominally  $1mm \times 1mm$  domain. Further details regarding the hot-wire processing may be found in Morris and Foss (2003). The four sensors were sampled at 20 KHz. Thus, a microdomain is created and the  $\omega_z$  is determined every  $50\mu s$ . The probe orientation, for this investigation, was such that the transverse direction was "z". Hence, the four-sensor probe provides  $u, v$ , and  $\omega_z$  time series. This orientation was selected for the  $I=0,1$  conditioning signal given that the time mean orientation of the VSL vorticity filaments were in the z-direction.

### THE I(T) ALGORITHM

The intermittency signal,  $I(t)$ , is constructed using a local standard deviation ( $\sigma$ ) of  $\omega_z$ . This  $\sigma$  value at a given time  $t$  is defined as:

$$\sigma(t) = \sqrt{\frac{1}{2\Delta t} \int_{t-\Delta t}^{t+\Delta t} (\omega_z(\tau) - \bar{\omega}_{z,m}(\tau))^2 d\tau} \quad (4)$$



\* – Gap for contraction boundary layer removal

Figure 1: The SSSL

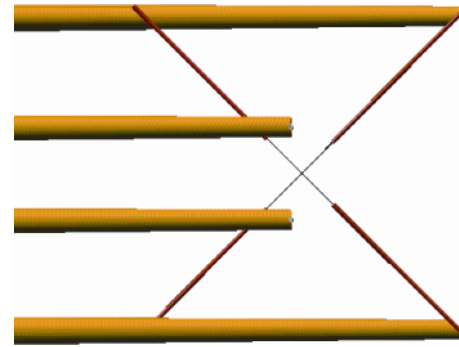


Figure 2: The Transverse Vorticity, or "Mitchell", probe

$$\bar{\omega}_{z,m}(t) \equiv \frac{1}{2\Delta t} \int_{t-\Delta t}^{t+\Delta t} \omega_z(\tau) d\tau \quad (5)$$

The  $\sigma$  value is computed for each timestep; a data rate of 20 kHz yields  $\sigma(t)$  with a timestep of  $50\mu s$ . The  $\Delta t$  used for the present data was equal to 60 timesteps, or 3 ms. This corresponds to approximately twice the Taylor time scale ( $\lambda_v$ ) in the most "active" part of the flow field. An example of this  $\sigma$  at  $\eta = 2.50$ ,  $x/\theta_0 = 200$  is shown in Figure 3.

Clearly, some non-zero threshold must be set such that values of  $\sigma$  greater than this value are deemed "active". This was done by analyzing  $\omega_z(t)$  in the free stream. Measured values of  $\sigma$  at this location can be regarded as a "calibration"

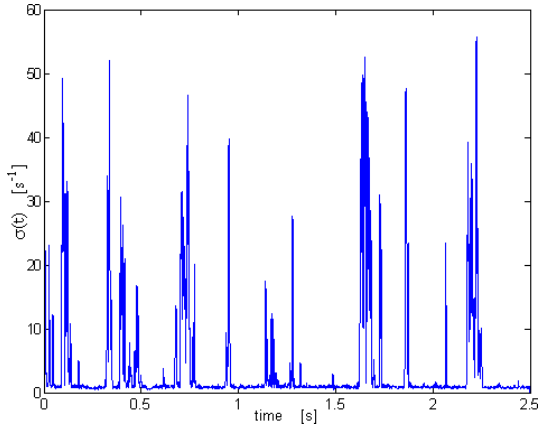


Figure 3:  $\sigma(t)$  at  $x/\theta_0 = 200$ ,  $\eta = 2.50$

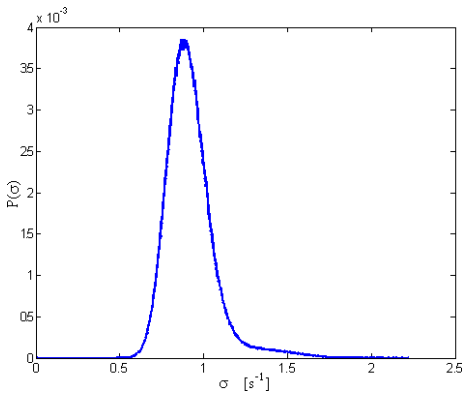


Figure 4: PDF of  $\sigma$ ,  $x/\theta_0 = 200$ ,  $\eta = 5.29$

of the measurement system that provides  $\omega_z(t)$  as well as the residual spanwise vorticity in the free stream. That is, since the free stream should be "inactive", the maximum computed value for  $\sigma$  in the free stream should be the threshold for activity. A PDF displaying the set of measured values at this location is shown in Figure 4.

A magnified view of  $\sigma$  along with  $\omega_z(t)$  is shown in Figure 5. Note that there is a portion of the  $\sigma$  signal which exceeds the selected threshold but which should not be considered "active". To ensure that such "false positives" do not occur, a "dwell" parameter is used. That is, the signal must be above or below the determined threshold for at least this length of time for the value of  $I(t)$  to change state. As in Hellum (2006),  $2\lambda_v(\eta)$  was used as this dwell parameter, where  $\lambda_v(\eta)$  is the Taylor microscale based on  $v(t)$ .

### CONDITIONAL STATISTICS

Conditional statistics can be defined as follows: "Given a set of observations for which condition A holds, what is the value of statistical measure B?" For example, one may be interested in the standard deviation (measure) of the  $u$  component of velocity during the active (condition) portion of the record.

The first conditional measure is the fraction of time that an "active" flow state is present at a given location. This value is termed  $\langle I \rangle$  and its distribution at  $x/\theta_0 = 200, 500$  is presented in Figure 6. Note the elevated values of  $\langle I \rangle$  near  $\eta = 0$  at  $x/\theta_0 = 200$  compared to the values at  $x/\theta_0 = 500$ .

This difference between  $\langle I \rangle$  at  $x/\theta_0 = 200$  and  $x/\theta_0 = 500$  is one of the principle effects of flow scale (or

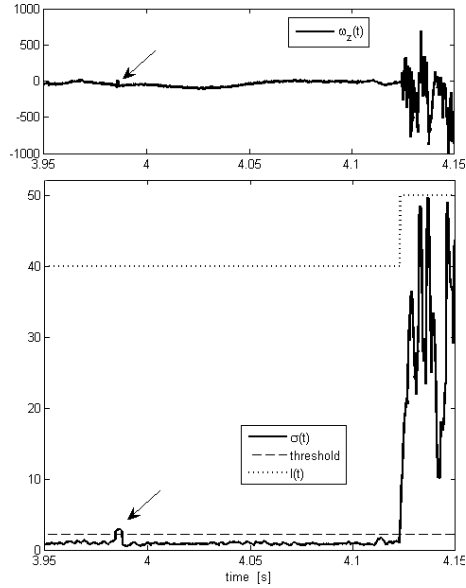


Figure 5:  $\sigma(t)$  at  $x/\theta_0 = 200$ ,  $\eta = 2.50$ , closeup. Note the "too short" region near 3.98 s.

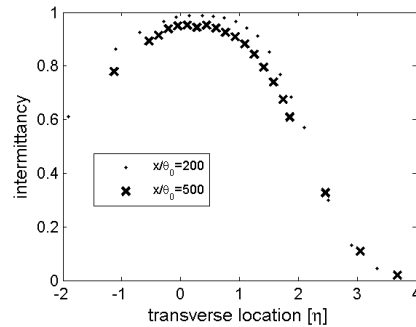


Figure 6:  $\sigma(t)$  at  $\eta = 2.50$ , zoomed-in.

evolution of the shear layer) that was observed in this investigation. Phillips (1972) describes a model of the vsl in which "wedges" of exterior fluid intrude into the region of the flow field most commonly occupied by sheared or interior fluid. Figure 6 indicates that a greater number of or deeper wedges exist at larger  $x/\theta_0$ . It is reasonable to postulate that the increase in vortical fluid that results from viscous diffusion (see Equation 1) lags behind the overall growth of the shear layer ( $d\theta/dx = 0.035$ ). This would have to be tested by further measurements downstream.

The mean  $u$  component of velocity at both  $x/\theta_0 = 200$  and  $x/\theta_0 = 500$  is presented in Figure 7. The top set of axes represents the unconditioned variable, the middle set represents the active condition, and the lowest set the inactive condition. It is apparent that, at least in the measure of the mean velocity distribution, that the flow is self-preserving by  $x/\theta_0 = 200$ . This observation is in agreement with the more extensive measurements of Morris and Foss (2003). Note the relatively larger gradient for the inactive condition near  $\eta = 0$ . This is reasonable, since most of the inactive fluid near the high-speed free stream ( $\eta > 0$ ) comes from the high-speed stream. Similarly, most of the inactive fluid near the entrainment stream ( $\eta < 0$ ) comes from the entrainment stream. With the exception of the inactive condition around  $\eta = 0$ , there is very little influence of the downstream distance on these x-component velocity results.

The standard deviations (SD) of the x and y component

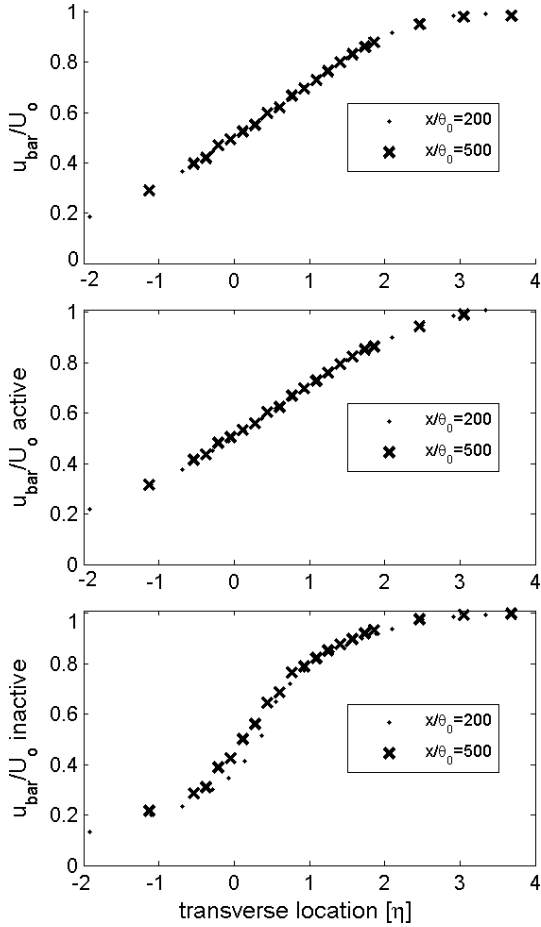


Figure 7:  $\bar{u}$ , unconditioned, active and inactive conditions

velocity fluctuations provide a similar message; see Figures 8 and 9. The top set of axes represents the unconditioned variable, the middle set represents the active condition, and the lowest set the inactive condition. Given that the SD indicates the width of the component's pdf, fluid arriving at a point with different magnitudes determines the SD value. The "active" SD values are relatively constant across the shear layer which indicates strong "mixing" of the interior fluid. Conversely, the "inactive" SD values exhibit low values at the shear layer edges but values which exceed the "active" fluid in the central region. This is readily understood to indicate that the velocities of the "exterior" fluid elements, from the two potential streams, are relatively unchanged even if they exist far from the region of their origin.

This interpretation is strengthened by observing the  $u'$ ,  $v'$  joint histograms at three lateral locations; see Figure 10. It is apparent that high-speed side inactive fluid ( $u' > 0$ ,  $v' < 0$ ) is present and "time-shared" with low-speed side inactive fluid ( $u' < 0$ ,  $v' > 0$ ) at  $\eta = 0.363$ .

The correlation of the velocity fluctuations ( $\overline{u'v'}$ ) is instructive regarding the kinematics of the flow as well as describing the Reynolds shear stress. The normalized quantity  $\overline{u'v'}/U_0^2$  at  $x/\theta_0 = 200$  and  $x/\theta_0 = 500$  is presented in Figure 11. The relatively flat profile of the active fluid compared to the inactive fluid is further justification for the "two-process" hypothesis described above.

The correlation coefficient ( $-\overline{u'v'}/\bar{u}\bar{v}$ ) at  $x/\theta_0 = 200$  and  $x/\theta_0 = 500$  is presented in Figure 12. The high magnitude ( $\approx -0.8$ ) values for this quantity for the inactive condition near the shear layer center represents a high correlation be-

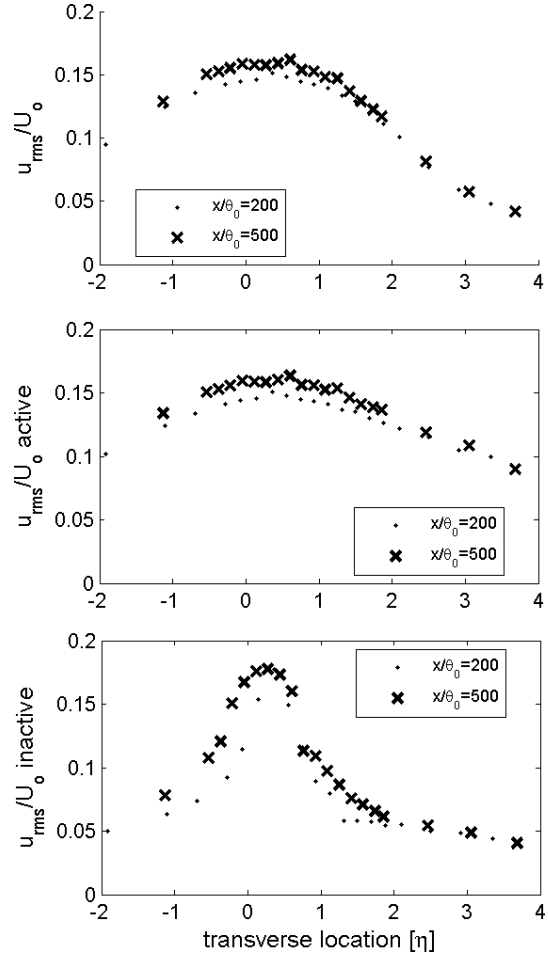


Figure 8:  $\bar{u}$ , unconditional, active and inactive conditions.

tween  $u$  and  $v$  fluctuations. This is again seen as a validation for the "two-process" hypothesis proposed above.

## COMPARISONS TO THE OBSERVATIONS OF WYGANSKI AND FIEDLER (1970)

The pioneering study by Wyganski and Fiedler (1970) (W&F) offers the opportunity to compare the detailed features of the two single stream shear layers. However, it is important to explicitly note the dissimilar features of the two flow systems. Namely:

1. The thin boundary layer was "tripped" near the separation lip for W&F. The present study developed a boundary layer [ $R_\theta = 4.40 \times 10^4$ ] that separated at the trailing edge.
2. In the present study, the entrainment fluid was introduced at a large distance ( $\Delta y \approx 3m$ ) from the separation lip in contrast with the screened and inclined surface that was nominally one shear layer width from the low-speed edge for W&F.
3. The present study utilized  $\omega_z(t)$  for its I=0,1 discrimination vs. the above noted processing of  $u(t)$  for W&F.

With these differences noted, several direct comparisons can be made. Note that the  $\bar{u}/U_0$  distribution of W&F was compared to that of the present data so that the W&F data could be scaled by an inferred  $\theta$ .  $\langle I \rangle$  as found by W&F and the present authors is shown in Figure 13. Note that

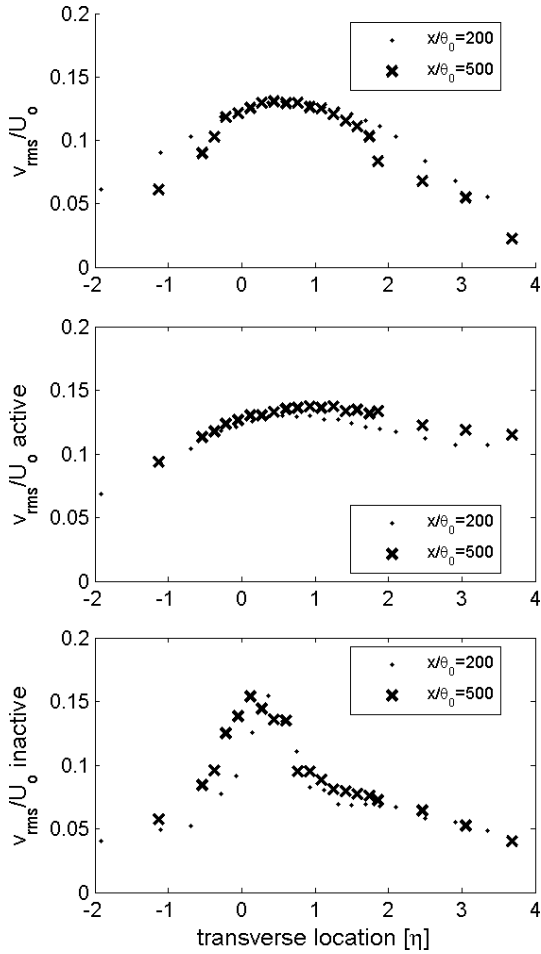


Figure 9:  $\bar{v}$ , unconditional, active and inactive conditions.

despite the distinct difference in the location of peak  $\langle I \rangle$ , the gradient of  $\langle I \rangle$  on the high speed side is quite similar. The observed difference in the relative "breadth" of the data sets' peaks may result from the different way the entrainment stream was treated in each facility.

Values of  $\bar{u}/U_0, \bar{v}/U_0$  found by W&F and the present authors are shown in Figure 14. Values of  $\overline{u'v'}/U_0^2$  found by W&F and the present authors are shown in Figure 15.

## SUMMARY

The defining quantity, for the binary intermittency (I) states of 1 and 0, was selected as the "activity" level of the spanwise vorticity signal:  $\omega_z(t)$ . Namely, when the locally defined standard deviation ( $\sigma$ ) exceeded a threshold level of  $2.21 \text{sec}^{-1}$  for the passage of nominally two Taylor microscales, the I value was set to 1. This definition, and its converse for  $I=0$ , provided a well defined conditioning signal for the development of conditional statistics.

The principal difference between the conditional values at  $x/\theta_0 = 200$  and  $x/\theta_0 = 500$  was the central region's mean values of the intermittency function. The lesser values at  $x/\theta_0 = 500$  indicate a stronger presence of the "wedges" of exterior fluid near the center of the shear layer at the downstream station. The first and second moments of the velocity fluctuations as well as the  $(u',v')$  correlations exhibited small variations between the two  $x/\theta_0$  locations.

## REFERENCES

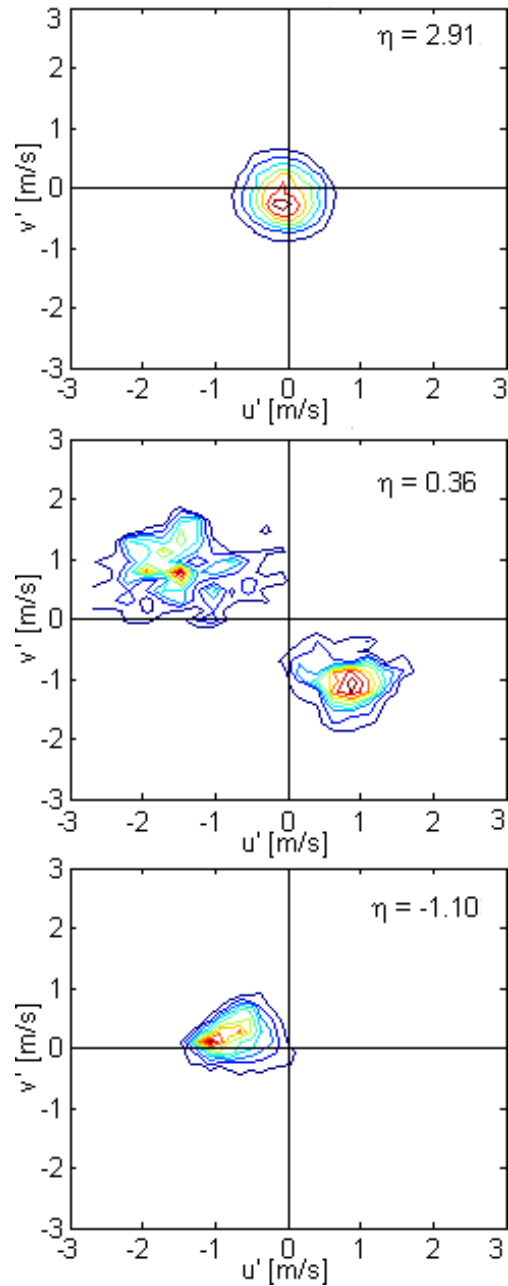


Figure 10: Joint PDFs of  $u'$  and  $v'$ , inactive condition, at  $x/\theta_0 = 200$

Corrsin, S and Kistler, A.L. (1955). "Free Stream Boundaries of Turbulent Flows". Nat'l Advisory Committee for Aeronautics, Report 1244.

Haw, R.C., Foss, J.K., and Foss, J.F. (1989) "Vorticity Based Intermittency Measurements in a Single Stream Shear Layer". *proc. Second European Turbulence Conference, Advances in Turbulence 2*, ed. Fernholz, H.H., and Fiedler, H.E.. Springer-Verlag, Berlin.

Hedley, T.B., and Keffer, J.F. (1974). "Turbulent/Non-turbulent decisions in an intermittent flow". *Journal of Fluid Mechanics*, Vol. 64, pp. 625-644

Hellum, A.M. (2006). "Intermittency and the Viscous Superlayer in a Single Stream Shear Layer". MS Thesis, Michigan State University.

Morris, S.C. and Foss, J.F. (2003). "Turbulent boundary layer to single stream shear layer: the transition region".

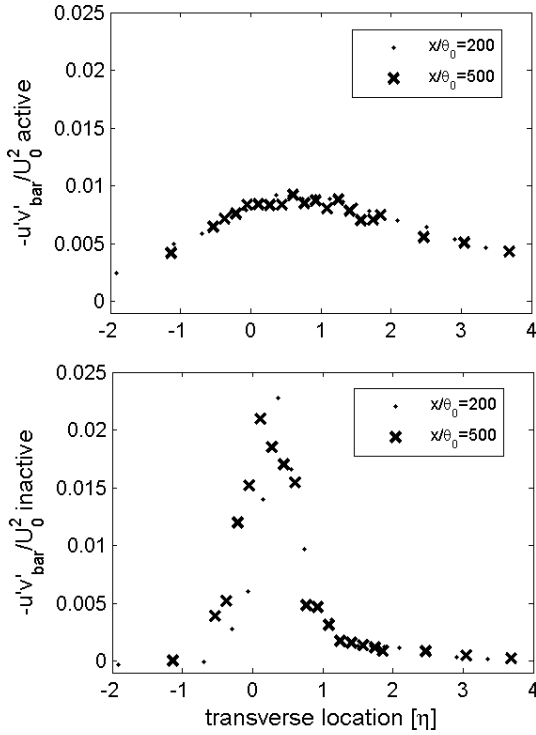


Figure 11:  $\overline{u'v'}/U_0^2$ , active and inactive conditions.

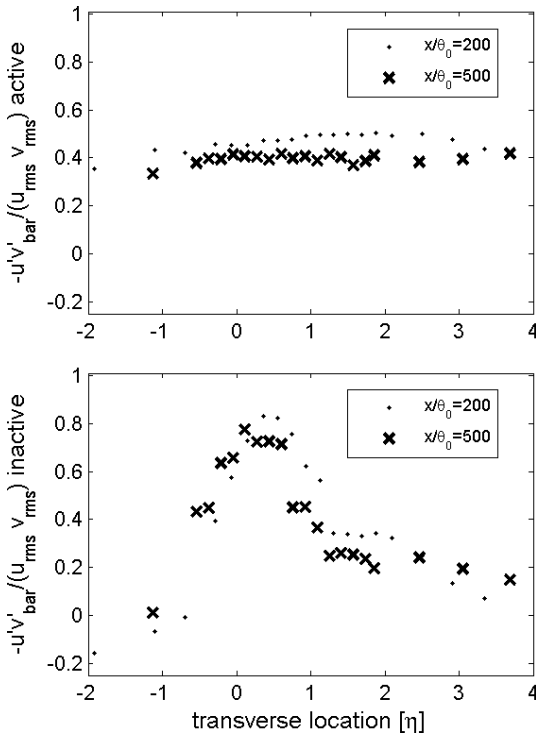


Figure 12:  $\frac{\overline{u'v'}}{\overline{u_rms v_rms}}$ , active and inactive conditions.

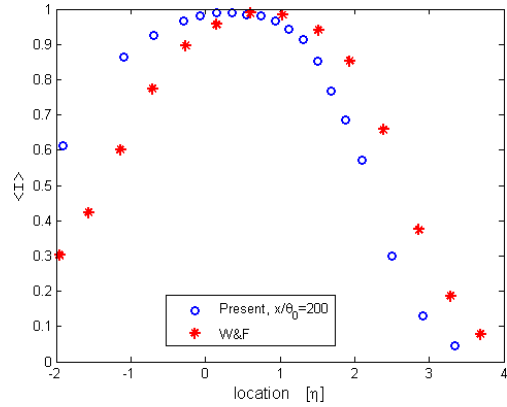


Figure 13: Comparison between  $\langle I \rangle$  of W&F and present data.

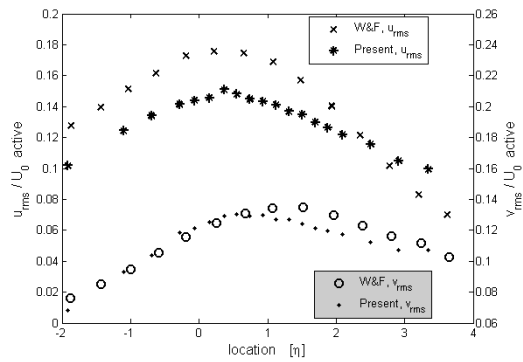


Figure 14: Comparison between  $\tilde{u}/U_0, \tilde{v}/U_0$  of W&F and present data.

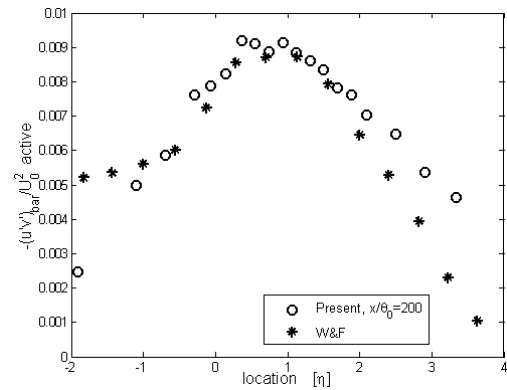


Figure 15: Comparison between  $\overline{u'v'}/U_0^2$  of W&F and present data.

*JFM*, Vol. 494, pp. 187-221.

Phillips, O.M. (1972). "The entrainment interface". *JFM*, Vol. 51, pp. 97-128.

Townsend, A.A. (1956). *The structure of Turbulent Shear Flows*, Cambridge University Press.

Wallace, J.M. and Foss, J.F. (1995). "The Measurement of Vorticity in Turbulent Flows", *Annual Reviews of Fluid Mechanics*, January.

Wynanski, I. and Fiedler H.E. (1969). "Some measurements in the self-preserving jet" *JFM*, Vol. 38, pp. 577-612.

Wynanski, I. and Fiedler H.E. (1970). "The two-dimensional mixing region". *JFM*, Vol. 41, pp. 327-361.